

Short Communication

Influence of aging time on properties of passive film formed on chromium in 0.05 M H₂SO₄

Yuchen Li, Fan Zhou, Ying Ren, Genshu Zhou*

State Key Laboratory for Mechanical Behavior of Materials, Xi'an Jiaotong University, Xi'an 710049, China

*E-mail: zhougs@mail.xjtu.edu.cn

Received: 25 July 2022 / Accepted: 25 August 2022 / Published: 10 September 2022

Potentiostatic test is an important measurement in electrochemical analysis to better comprehend the electrode processes and corrosion mechanism. Aging of thin passive films is typically characterized by curve of steady state current density (I_{ss}) versus time (t). However, the initial current spike could not be explained by using the existing models of passivity. In this study, electrochemical method and X-ray photoelectron spectroscopy combined with Ar⁺ ion sputtering were used for the analysis of current response and variation of film composition during aging. It was believed that electronic conduction was predominant due to electron tunneling at the initial stage, and the decay of steady state current density was controlled by the chemical dissolution of Cr³⁺ at film/solution interface.

Keywords: Passive film, XPS, Chromium, Steady state current, Electrochemical analysis.

1. INTRODUCTION

Dynamic polarization test is one of the most important methods in electrochemical analysis to better comprehend the electrode processes and corrosion mechanism. The current-voltage (I - V) relationship can be further analyzed by current-time (I - t) response under potentiostatic test. For the passivity of metal, the I - t response is called aging, which is a special kinetic phenomenon. It was first proposed by Sato and Cohen in their study on aging of anodic oxide film on iron.[1] When an over potential is applied on the passive film, the film properties, such as composition, microstructure, and ionic or electronic conductivity, can undergo significant variation with time.[2] A typical electrochemical characterization on aging is the change of steady state current density (I_{ss}) with time (t). In this process, the current first increases instantaneously and then decreases rapidly, followed by a very slow stabilization.

In the earlier studies on the growth of passive films, the delay of current was interpreted as the decrease of growth rate. It was proven later by *ex situ* angle-dependent X-ray photoelectron spectroscopy

(XPS) and *in situ* electrochemical quartz crystal microbalance (EQCM) measurement for the passivity behavior of pure Chromium (Cr).[3, 4] However, this interpretation is only a brief description, and further details on the current, including constituent variation and conducting property, are vague and less investigated. Kirchheim and coworkers believed that the total current for the passive film on iron (Fe) was the combination of formation current and corrosion current, and the decrease of the over potential at film/solution interface led to the decrease of the two types of currents.[5, 6] However, this did not separate the metal oxidation part for direct dissolution in solution from the corrosion part of chemical dissolution. Olsson and coworkers studied the thickness change of the passive film on Cr during potential sweep by *in situ* EQCM measurement, and indicated that the current consisted of the film formation part and the metal dissolution part, and the decrease of the relative proportion of formation current with time was due to the decrease of the electric field in the film.[7] For the passive film on zinc (Zn), the delay of current was explained as a result of the decrease of defects concentration due to cation–anion recombination.[8] The current spike was observed to be accompanied by a significant increase of metal dissolution.[4, 7, 9]

In terms of the conduction property of passive films on Fe, Cr, nickel (Ni), 316L stainless steel, *etc.*, electronic conduction has been supported by some researchers, largely due to the argument that the passive film is semi-conductive, and the film formed is in depletion state.[2, 10-14] However, it cannot account for why the Faradic current that contributes to the growth of the passive film, is generated by the applied potential in passive range.[15] Moreover, the ionic conduction has been supported by some others, because the growth of passive film depends on the ion and ionic defects transfer.[5, 16-18] For the ionic conduction, however, the current spike during the initial period cannot be explained, and this is less noticed.[18] It is possible that the passive film is a mixed ionic electronic conductor. However, it is crucial to determine which conduction type dominates during aging, because the type of conduction can aid in determining the potential drop in the film and further evaluating the rate-limiting step of growth.

The I_{ss} - t curve covers the entire process from growth at the initial phase to quasi-steady state in the subsequent phase. However, this typical curve is also observed under potentials in both cathodic range and transpassive range. Therefore, it may contain something in common among each polarized range. Besides, the conduction property of passive films was first determined, as it is the analytical presupposition on the change in current. In this study, an electrochemical method based on the transformation of alternating-current impedance was adopted to study the initial unsteady stage which represented the film growth, and then XPS depth-profile analysis was combined to characterize the thickness, variation of valence state, and relative content of metal oxides in the quasi-steady stage. Pure Cr was used for the investigation.

2. EXPERIMENTAL

Pure polycrystalline chromium (purity 99.99%, Baosteel) was used for the investigation. The electrolyte for Cr electrode was aerated 0.05 M H₂SO₄ with pH 1 (analytical grade 97% H₂SO₄ and distilled water). Specimens were cut into cylinders with a diameter of 8 mm and height of 3 mm. A pure Cu wire was then attached to the back of each sample for making electrical connections with an external

circuit. Specimen and connecting wire were insulated with polytetrafluoroethylene, which allowed only the bottom circular face (area of 0.5 cm^2) to be exposed to the electrolyte. Before the experiment, the working electrode was polished with silicon carbide paper from grade 400 to grade 1500 and then thoroughly washed with deionized water.

Electrochemical tests were conducted in a three-electrode cell, equipped with a platinum counter electrode (area $10 \text{ mm} \times 10 \text{ mm} \times 2 \text{ mm}$) and a saturated mercurous sulfate reference electrode (MSE). All the electrode potentials were quoted on this electrode. Potentiostatic polarization was applied to form passive films to be investigated. An alternating voltage with an amplitude of 10 mV at 100 mHz was applied during the potentiostatic polarization to record the variation of impedance with time. All the electrochemical measurements were performed using an electrochemical workstation (IM6eX ZAHNER, Germany).

Two samples aged at -100 mV (the potential in a high passive range to avoid film change during transfer[19]), respectively, for 1 and 24 h were analyzed by XPS (ESCALAB Xi⁺, Thermo Fisher Scientific, USA) with Al K α radiation at source power of 400 W . The spot size on the sample was $500 \mu\text{m}$. The hemispherical sector analyzer for electron detection was operated in constant analyser energy mode with the pass energy for the high-resolution scans set to 20 eV . The step width of the energy channels was set at 0.05 eV . The sputter size was set to 2 mm . The thickness of the passive film was determined using an ion beam (raster 500 eV Ar^+) at a rate of $0.03 \text{ nm}\cdot\text{min}^{-1}$, which was calibrated by measuring the sputtering depth per minute in a standard specimen (Ta_2O_5). The base pressure of the ultra-high vacuum analysis chamber was in the low range of 10^{-10} mbar range. When the flood gun was applied, the pressure settled in the 10^{-7} mbar range. XPS binding energies were calibrated with reference to binding energy of C1s peak at 284.6 eV recorded from graphite. All spectra were fitted with Shirley background subtraction and peak deconvolution by using CASA XPS software.

3. RESULTS

Potentiostatic polarization was applied at different potentials according to the polarization curve of Cr in $0.05 \text{ M H}_2\text{SO}_4$ solution,[15] as shown in Figure 1.

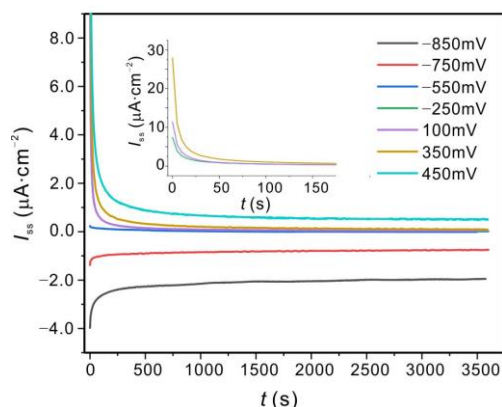
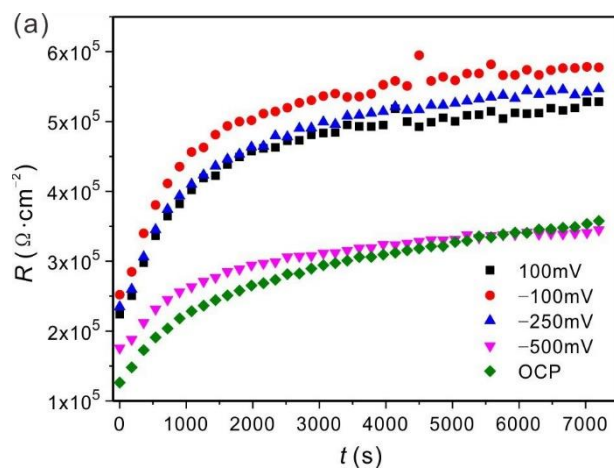


Figure 1. Potentiostatic curves of samples at different potential. The open circuit potential of samples stabilized at 600 mV in $0.05 \text{ M H}_2\text{SO}_4$ solution, and then different potentials were applied using potentiostatic polarization, respectively. The initial stage of the current is shown in the inset.

Current spike could be observed in each range, for example, the transpassive range (350 and 450 mV) and the cathodic range (-750 and -850 mV). However, noteworthy, I_{ss} in quasi-steady state in the passive range was the lowest, and it was independent of the applied potential. For the initial current spike, electronic double layer charging as suggested by some researchers,[7] was first excluded, because the potential scanning rate was extremely slow (no more than $100 \text{ mV}\cdot\text{s}^{-1}$) and could not give rise to such high response current. The inset in Figure 1 shows that the time constant would be up to several seconds if the current was regarded as charging current. Thus, the current spike was composed almost of Faradic current.

To further analyze the impedance change during the unsteady state, a small alternating voltage at 100 mHz (low-middle frequency impedance could reflect film resistance according to the electrochemical impedance spectroscopy (EIS) measurement on passive films) was imposed on the polarized sample, and then RC parallel circuit was selected to record the variation of film resistance, in a way similar to the capacitance–time measurement reported in our previous study.[15] Noteworthy, the resistance obtained does not represent the real resistance of passive film, however, it reflects the variation trend of resistance. Figure 2a demonstrates that the resistance increases rapidly at initial stage under each applied potential, and then the increasing rate slows down with time to a quasi-steady state, which is consistent with the variation of growth rate of film obtained by EQCM measurement.[4, 7] Noteworthy, the resistance in quasi-steady state was independent of potential in the passive range, which conformed to the results of I_{ss} mentioned above. Comparative analysis indicates that the resistance at open circuit potential (OCP) increased with a relatively slow rate, and the stabilized resistance was only half of that in passive range. For the film formed at -250 mV for 2 h with a steady state and high resistance, different potentials were applied subsequently (see Figure 2b). Notably, all the resistances suddenly dropped, and then rapidly increased with the exception of that at -450 mV. Combined with the current spike in $I_{ss}-t$ curve (Figure 1), both the film resistance and current showed a step response when the applied potential was changed, which indicates that the initial response could be related to electronic response rather than ionic migration.



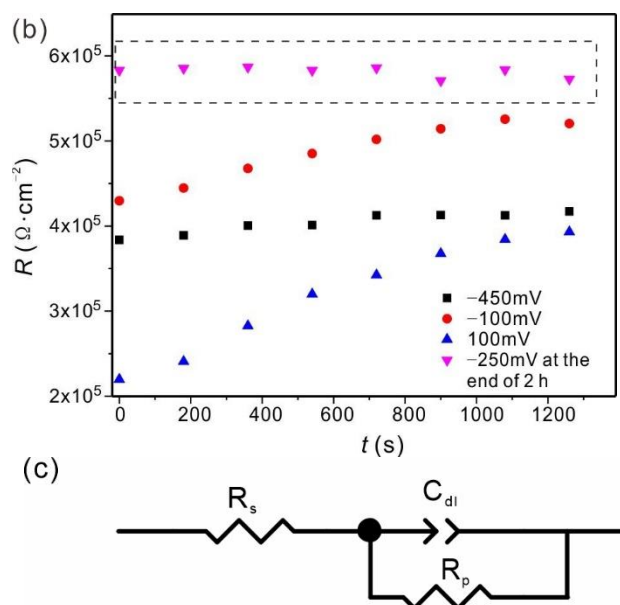


Figure 2. (a) Resistance as a function of aging time (15-min intervals) at different potentials. The resistance was obtained from fitting results of impedance using (RC) parallel circuit, (b) Resistance as a function of aging time (3-min intervals) at the initial stage when the applied potential was alternated from -250 mV to different potentials. The inverted triangle represents the resistance variation at the end of 2 h at -250 mV. A sudden drop of resistance can be observed when the applied potential is alternated, and (c) EIS equivalent circuit for fitting EIS curves shown in (a) and (b).

The electrochemical behavior of the passivity of pure Cr showed a continuous variation from the initial stage to the quasi-steady state, which consequently formed the passive film on the surface of Cr metal. In order to observe the change in chemical state along the depth profile during the process, *ex situ* XPS combined with Ar^+ ion etching was used for the film formed at -100 mV for 1 and 24 h, respectively. The Cr2p and O1s spectra during long time sputtering on the films are presented in Figure 3. Evidently, no significant change in peak shape occurred with the prolongation of the etch time, however, the intensity of some peaks gradually varied. A small shift between the surface spectrum and the subsequent spectra was observed in all the depth profiles, which was attributed to slightly different charge neutralization conditions on the surface.[20, 21] High-resolution spectra were analyzed by CasaXPS software (version2.3.13) to obtain the variation of valence state and relative content. Notably, Cr 2p_{3/2} spectrum could give rise to multiplet splitting, therefore, the fitting was based on multiplet split spectra according to literature studies.[22, 23] Some of the fitting results are shown in Figure 4, and all the numerical results were plotted versus etch time, as shown in Figure 5. For the unspattered surface (Figure 4a), the content of Cr metal from Cr2p spectrum was the highest, and the contents of Cr(OH)₃ and Cr₂O₃ were almost the same. However, the O 1s spectrum (Figure 4c) for the unspattered surface showed a high percentage of Cr(OH)₃, this might be due to the surface contamination from element O. The subsequent Cr(OH)₃/Cr₂O₃ ratio from O 1s spectrum (Figure 5b) showed a good consistency with that from Cr 2p_{3/2} spectrum (Figure 5a). Water was observed only on the unspattered surface, since it was removed during sputtering.[20]

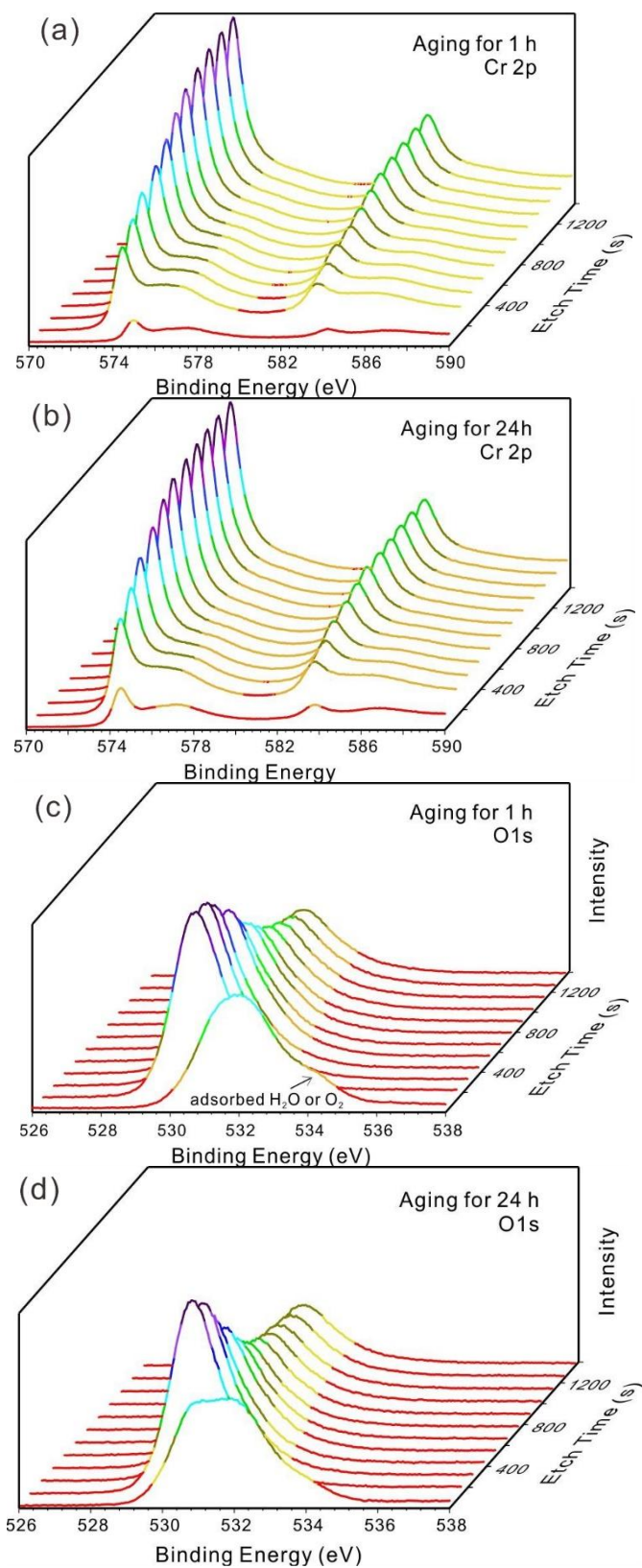


Figure 3. XPS depth profiles of the film formed at -100 mV for 1 h and 24 h, respectively. (a) Cr 2p spectra of the film formed at -100 mV for 1 h, (b) Cr 2p spectra of the film formed at -100 mV for 24 h, (c) O 1s spectra of the film formed at -100 mV for 1 h, and (d) O 1s spectra of the film formed at -100 mV for 24 h.

Several conclusions could be inferred from the results shown in Figure 5. Firstly, the content of $\text{Cr}(\text{OH})_3$ was less than that of Cr_2O_3 through the entire thickness of the film except the outer layer. Second, the $\text{Cr}(\text{OH})_3/\text{Cr}_2\text{O}_3$ ratio decreased significantly with thickness, while the content of Cr metal of more than 50% increased significantly with thickness. Third, the $\text{Cr}(\text{OH})_3/\text{Cr}_2\text{O}_3$ ratio declined with aging time, while O/Cr ratio decreased with aging time. The passive film on Cr was characterized in detail by angle-resolved XPS in previous study, showing that there was a certain amount of Cr metal in the passive film.[3] Similar results could also be found for passive films on alloys, however, more attention was paid to the variation of oxide/hydroxide ratio with time or thickness.[24-28] Herein, dehydration process with aging could also be observed, which resulted in the decrease of $\text{Cr}(\text{OH})_3/\text{Cr}_2\text{O}_3$ ratio. The content of Cr metal without etching did not vary with aging, it was thus indicated that they both have the same thickness. However, a content difference was observed during etching, which indicates the etch rates of the two differed due to the compactness of the film. Obviously, it can be attributed to the increase of Cr_2O_3 in film with aging.

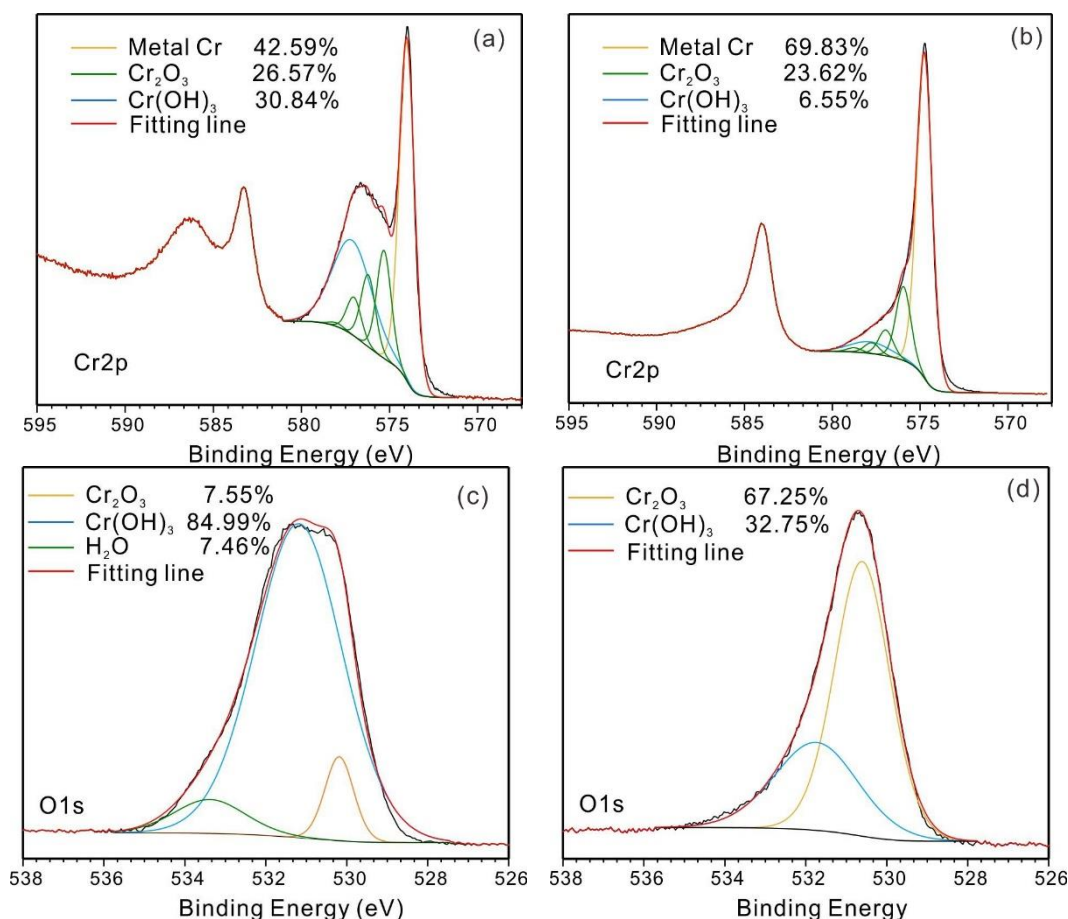


Figure 4. High-resolution scans of Cr2p and O1s and the corresponding fitting results. The resolved Cr2p region for the unspun surface of the film formed (a) for 24 h and (b) for a deeper level (after 1360 s sputter time), respectively. Furthermore, the resolved O1s region for the (c) unspun surface and (d) a deeper level (after 1360 s sputter time) of the film formed for 24 h, respectively.

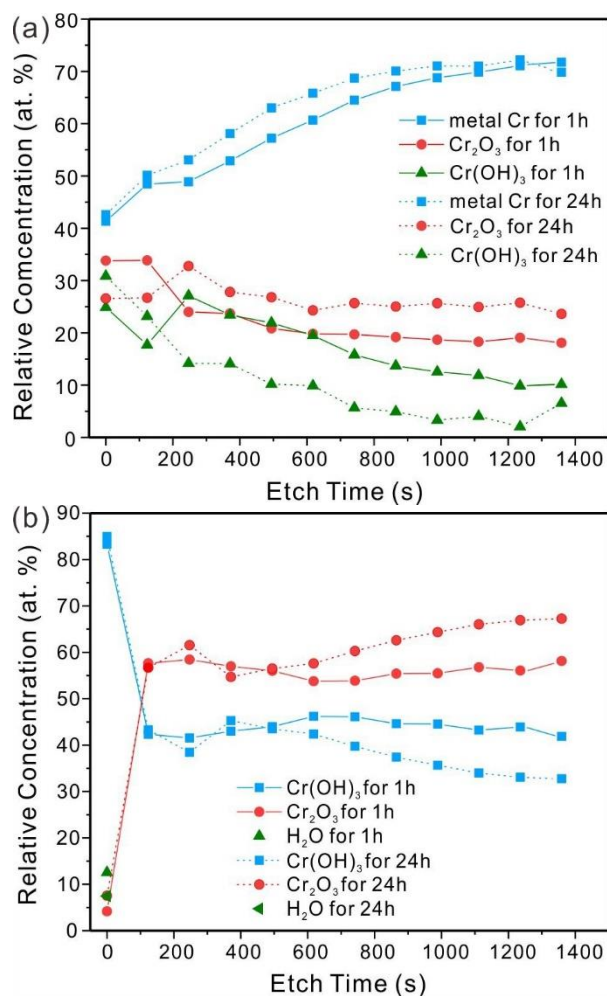


Figure 5. Composition variation as a function of etch time according to the fitting results from: (a) Cr2p spectrum and (b) O1s spectrum.

4. DISCUSSION

Figure 2b exhibits the step response of R , indicating that the film impedance at the initial polarization could be controlled by electronic mobility rather than ionic mobility in film, as ionic transfer requires a certain time at the interface. In other words, electron tunneling through the film (with a thickness less than 3 nm[29, 30]) predominated in this stage. Therefore, I_{ss} was controlled by Faradic reactions instead of ionic migration, which could be described via Butler-Volmer equation. The rate of the anodic reaction then rapidly decreased similar to the cathodic reactions at -850 and -750 mV; however, it could not be attributed to the limited mass transfer occurring on cathode[31]. With the increase in the film thickness with anodic reaction, the resulting increase of tunneling distance led to the rapid decrease in the reaction rate. However, noticeably, the steady-state current was highly metal-dependent.[32] Thus, the decrease due to Faradic reaction was then controlled by the chemical dissolution of Cr₂O₃. As the solubility of Cr₂O₃ was very low and constant in solution, the stabilized current did not change much with the increase of the applied potential[33]. In terms of the rate-limiting reactions at film/solution interface, film dissolution reactions were reported for the passivated iron in acid solution, indicating that the corrosion rate was dependent on the potential drop at the interface.[18,

34] It may be related to the complex valence of FeO_x (Fe^{2+} , Fe^{3+} and the mixture of the two) on Fe. For the passive film on Cr, however, only Cr^{3+} exists in the formed film, thus the dissolution reaction of the film is:



This reaction is potential independent, which conforms to our results in shown Figures 1 and 2 that I_{ss} and steady resistance are nearly independent of the applied potential in passive range. In the transpassive range, some Cr^{3+} was oxidized to Cr^{6+} due to potential that has large solubility in solution, thus leading to a jump of steady current density.

This was also confirmed by our XPS results of composition differences from aging. As I_{ss} decreases with aging and the resistance increases with aging, the remarkable variation is the decrease of the ratio of $\text{Cr}(\text{OH})_3/\text{Cr}_2\text{O}_3$. It is well known that the solubility of $\text{Cr}(\text{OH})_3$ is greater than that of Cr_2O_3 , thus the decrease of anodic reaction rate is attributed to the decrease of interfacial dissolution of Cr^{3+} (Equation (1)). Although the variation of composition is independent of potential, it is indicated that the dehydration of the passive film with aging should be related to the electric field established on the surface. This electric field could promote the migration of metal cations toward solution, and resulting in the formation of Cr_2O_3 .

Therefore, by combining electrochemical response and composition variation, the aging current on Cr surface can be determined by following two factors: in the initial stage, anodic reaction and the formation of passive film on the metal surface take place simultaneously, thus the current spike is controlled by electron transfer, and the following decrease is due to the increase of tunneling distance of electrons resulting from the formation of passive film. Then the decrease arrives at a platform, where a dynamic balance between electrochemical reaction (film growth) and chemical dissolution of Cr^{3+} is achieved so as to maintain the film thickness. The current platform shows a very slow decline due to the decrease of the ratio of $\text{Cr}(\text{OH})_3/\text{Cr}_2\text{O}_3$ during aging.

5. CONCLUSION

The current change of the passive film on Cr during aging was analyzed in terms of current, resistance, and film composition by potentiostatic polarization. The step response of both film resistance and current at initial stage indicates that electronic conduction predominated in the film, which could be described by Faradic reactions via electron tunnelling at film/solution interface. The subsequent slow decay of the current was due to the limited dissolution of Cr^{3+} which was independent of potential in passive range. This was confirmed by the XPS depth profiling result on the passive film undergoing dehydration process during aging. The anodic reaction rate decreased slowly with aging due to the increase of Cr_2O_3 in film instead of thickness, showing the occurrence of solubility-controlled electrochemical process at film/solution interface in the following steady-state stage.

CONFLICT OF INTEREST

No conflict of interest exists.

ACKNOWLEDGEMENTS

□ This work is supported by the Science and Technology Innovation Program of Xi 'an (No.: 201805064ZD15CG48) and Key Research and Development Program of Shaanxi Province (No.:

2021GY-253). The authors acknowledge Ms Jiamei Liu, Instrument Analysis Center of Xi'an Jiaotong University, for the XPS measurements.

References

1. N. Sato, M. Cohen, *J. Electrochem. Soc.*, 111 (1964) 624.
2. P. Schmuki, *J. Solid State Electrochem.*, 6 (2002) 145.
3. V. Maurice, W.P. Yang, and P. Marcus, *J. Electrochem. Soc.*, 141 (1994) 3016.
4. C.-O.A. Olsson, D. Hamm, and D. Landolt, *J. Electrochem. Soc.*, 147 (2000) 4093.
5. R.Kirchheim, *Electrochim. Acta.*, 32 (1987) 1619.
6. R.Kirchheim, B.Heine, H.Fischmeister, S.Hofmann, and U.S. H.Knote, *Corros. Sci.*, 29 (1989) 899.
7. C.O.A. Olsson, D. Hamm, and D. Landolt, *J. Electrochem. Soc.*, 147 (2000) 2563.
8. C.V. DAlkaine, M.N. Boucherit, *J. Electrochem. Soc.*, 144 (1997) 3331.
9. D. Hamm, K. Ogle, C.O.A. Olsson, S. Weber, and D. Landolt, *Corros. Sci.*, 44 (2002) 1443.
10. S.P. Harrington, T.M. Devine, *J. Electrochem. Soc.*, 156 (2009) C154.
11. M.A. Rodriguez, R.M. Carranza, *J. Electrochem. Soc.*, 158 (2011) C221.
12. B. Ter-Ovanesian, C. Alemany-Dumont, and B. Normand, *Electrochim. Acta*, 133 (2014) 373.
13. M.S. F. Di Quarto, *Corro. Eng. Sci. Techn.*, 39 (2004) 1.
14. T. Massoud, V. Maurice, F. Wiame, L.H. Klein, A. Seyeux, and P. Marcus, *J. Electrochem. Soc.*, 159 (2012) C351.
15. Y. Ren, G. Zhou, *J. Electrochem. Soc.*, 164 (2017) C182.
16. D.D. Macdonald, M. Urquidimacdonald, *J. Electrochem. Soc.*, 137 (1992) 2395.
17. C. Boissy, C. Alemany-Dumont, and B. Normand, *Electrochem. Commun.*, 26 (2013) 10.
18. K.J. Vetter, *Electrochim. Acta*, 16 (1971) 1923.
19. C.Courty, H.J.Mathieu, and D.Landolt, *Electrochim. Acta*, 36 (1991) 1623.
20. R. Steinberger, J. Duchoslav, M. Arndt, and D. Stifter, *Corros. Sci.*, 82 (2014) 154.
21. G. Greczynski, L. Hultman, *Prog. Mater Sci.*, 107 (2020) 100591.
22. M.C. Biesinger, C. Brown, J.R. Mycroft, R.D. Davidson, and N.S. McIntyre, *Surf. Interface Anal.*, 36 (2004) 1550.
23. M.C. Biesinger, B.P. Payne, A.P. Grosvenor, L.W.M. Lau, A.R. Gerson, and R.S. Smart, *Appl. Surf. Sci.*, 257 (2011) 2717.
24. Z.C. Feng, X.Q. Cheng, C.F. Dong, L. Xu, and X.G. Li, *Corros. Sci.*, 52 (2010) 3646.
25. B. Elsener, D. Addari, S. Coray, and A. Rossi, *Electrochim. Acta*, 56 (2011) 4489.
26. Z.J. Zheng, Y. Gao, Y. Gui, and M. Zhu, *J. Solid State Electrochem.*, 18 (2014) 2201.
27. J. Jayaraj, D.N.G. Krishna, C. Mallika, and U.K. Mudali, *Mater. Chem. Phys.*, 151 (2015) 318.
28. K.S. Wang, S. Tong, and M.K. Lei, *J. Electrochem. Soc.*, 162 (2015) C601.
29. E. Hamada, K. Yamada, M. Nagoshi, N. Makiishi, K. Sato, T. Ishii, K. Fukuda, S. Ishikawa, and T. Ujio, *Corros. Sci.*, 52 (2010) 3851.
30. L. Wang, A. Seyeux, and P. Marcus, *Corros. Sci.*, 165 (2020) 108395.
31. K. Tesař, K. Balík, *Mater. Today*, 35 (2020) 195.
32. J. Sun, H. Tang, C. Wang, Z. Han, and S. Li, *Steel Res. Int.*, 93 (2022) 2100450.
33. S. Zhang, Y. Li, C. Wang, and X. Zhao, *Int. J. Electrochem. Sci.*, 14 (2019) 91.
34. K.J. Vetter, F. Gorn, *Electrochim. Acta*, 18(4) (1973) 321.